

Do You Really Mean That? Content Driven Audio-Visual Deepfake Dataset and Multimodal Method for Temporal Forgery Localization

Zhixi Cai¹, Kalin Stefanov¹, Abhinav Dhall^{2,1} and Munawar Hayat¹

{zhixi.cai,kalin.stefanov,munawar.hayat}@monash.edu,abhinav@iitrpr.ac.in

¹Monash University and ² Indian Institute of Technology Ropar

¹Australia and ² India

ABSTRACT

Due to its high societal impact, deepfake detection is getting active attention in the computer vision community. Most deepfake detection methods rely on identity, facial attribute and adversarial perturbation based spatio-temporal modifications at the whole video or random locations, while keeping the meaning of the content intact. However, a sophisticated deepfake may contain only a small segment of video/audio manipulation, through which the meaning of the content can be, for example, completely inverted from sentiment perspective. To address this gap, we introduce a content driven audio-visual deepfake dataset, termed as Localized Audio Visual DeepFake (LAV-DF), explicitly designed for the task of learning temporal forgery localization. Specifically, the content driven audio-visual manipulations are performed at strategic locations in order to change the sentiment polarity of the whole video. Our baseline method for benchmarking the proposed dataset is a 3DCNN model, termed as Boundary Aware Temporal Forgery Detection (BA-TFD), which is guided via contrastive, boundary matching and frame classification loss functions. Our extensive quantitative analysis demonstrates the strong performance of the proposed method for both tasks of temporal forgery localization and deepfake detection.

KEYWORDS

Datasets, Deepfake, Localization, Detection

1 INTRODUCTION

Advances in computer vision and deep learning methods (e.g. Autoencoders [54] and Generative Adversarial Networks [19]) have enabled the creation of very realistic fake videos, known as *deepfakes*¹. There are various ways of creating deepfakes, including voice cloning [27, 65], face reenactment [52, 63], and face swapping [34, 49]. Highly realistic deepfakes are a potential tool for spreading harmful misinformation given our increasing online presence. This success in generating high quality deepfakes has raised serious concerns about their role in shaping people’s beliefs with some scholars suggesting that deepfakes are a “threat to democracy” [5, 55, 56, 62]. As an example of the potentially harmful effect of deepfakes, consider the recent work [61] that uses video of the former United States President Barack Obama to showcase a novel face reenactment method. In this work, the lip movements of Barack Obama are synchronised with another person’s speech, resulting in high quality and realistic video in which the former president appears to say something he never did. Given the recent surge in

¹In the text, *deepfake* and *forgery* are used interchangeably.



Figure 1: Content driven audio-visual manipulation. On the left is a real video with the subject saying “Vaccinations are safe”. On the right is audio-visual deepfake created from the real video based on the change in perceived sentiment where “safe” is changed to “dangerous”. Green-edge and red-edge images are real and fake frames, respectively. Through a subtle audio-visual manipulation, the complete meaning of the video content has changed.

synthesized fake video content on the Internet, it has become increasingly important to identify deepfakes with more accurate and reliable methods. This has led to the release of several benchmark datasets [16, 33, 53] and methods [43] for fake content detection. These fake video detection methods aim to correctly classify any given input video as either *real* or *fake*. This suggests that the major assumption behind those datasets and methods is that fake content is present in the entirety of the video/audio signal, that is, there is some form of manipulation throughout the content. And current state-of-the-art deepfake detection methods [14, 24, 66] achieve impressive results on this problem using the largest benchmark datasets.

However, fake content might constitute only small part of an otherwise long real video, as it was initially suggested in [11]. Such short modified segments have the power to completely alter the meaning and sentiment of the original real content. As an example, consider the manipulation illustrated in Figure 1. The real video might represent a person saying “Vaccinations are safe”, while the fake includes only a short modified segment, for example “safe” is replaced with “dangerous”. Hence, the meaning and sentiment of the fake video are significantly different from the real. This type of coordinated manipulation, if done precisely, has the potential to sway public opinion (e.g. when employed for media of a popular person as the example with Barack Obama) in a particular direction, for example, based on target sentiment polarity. Given the discussed major assumption behind current datasets and methods, the state-of-the-art deepfake detectors might not perform well on this type of manipulations.

Inspired by this idea and observation, in this paper we tackle the identified important task of detecting content altering fake segments in videos. The literature review on benchmark datasets for deepfake detection indicates that there is no dataset suitable for this task, that is, dataset that consists of content driven manipulations. Therefore, in this paper, we describe the process of creating such large-scale dataset that will enable further research in this important direction. In addition, we propose a novel multimodal method for precise prediction of the boundaries of fake segments based on visual and audio information. The **main contributions** of our work are as follows:

- (1) We introduce a new large-scale public audio-visual dataset, called *Localized Audio Visual DeepFake (LAV-DF)*, explicitly designed for the task of temporal forgery localization of content driven manipulations.
- (2) We propose a new multimodal method, called *Boundary Aware Temporal Forgery Detection (BA-TFD)* for audio-visual temporal forgery localization of content driven manipulations.

2 RELATED WORKS

Deepfake Datasets. The body of research in deepfake detection is driven by seminal datasets curated with different manipulation methods. A summary of the relevant datasets is presented in Table 1. Korshunov and Marcel [33] curated one of the first deepfake datasets DF-TIMIT, where face-swapping was performed on Vid-Timit. Down the lane, other important datasets such as UADFV [68], FaceForensics++ [53], and Google DFD [48] were introduced. Due to the complexity of face manipulation and limited availability of open-source face manipulation techniques, these datasets are fairly small in size [38]. Facebook released a large sized dataset DFDC [16] in 2020 for the task of deepfake classification. Multiple face manipulation methods were used to generate a total of 128,154 videos including real videos of 3000 actors. DFDC [16] has become a mainstream benchmark dataset for the task of deepfake detection. With the progress in both audio and visual deepfake manipulation, post DFDC, several new datasets as Celeb-DF [38], DeeperForensics [28], and WildDeepFake [71] were introduced. It is worth noting that all these datasets are designed for the binary task of deepfake classification and focus primarily on visual manipulation detection [11]. In 2021, OpenForensics [35] dataset was introduced for spatial detection and segmentation. Bounding boxes and masks are provided for each video along with real or fake labels. The number of faces in each frame is more than one. Recently, FakeAVCeleb [31] was released focusing on both face-swap and face-reenactment methods with manipulated audio and video. ForgeryNet[23] is the latest contribution to the growing list of deepfake detection datasets. This large-scale dataset is also centered around video-only identity manipulation and is suitable for the tasks of video/image classification and spatial/temporal forgery localization.

To the best of our knowledge, all these previous datasets assume that face manipulation occurs in most of the frames of the video [11]. Only the latest one, ForgeryNet [23], provides examples of the important problem of temporal forgery localization since it includes random face swapping applied to parts of some videos. However, the manipulations present in that dataset are only identity modifications that do not necessarily alter the meaning of the content.

Our content driven manipulation dataset LAV-DF addresses this important gap.

Deepfake Detection. Deepfake detection methods draw inspiration from observations of artifacts such as different eye colors, unnatural blink and lip-sync issues in deepfake videos. These binary classification methods are based on both traditional machine learning methods (e.g. EM [21] and SVM [69]) and deep learning methods (e.g. 3DCNN[15], GRU[45] and ViT [14, 24, 66]). Previous methods [20, 36] also aim to detect temporal inconsistencies in deepfake content and recently, several audio-visual deepfake detection methods such as MDS [11] and M2TR [64] were proposed. The methods above are classification centric and do not focus on temporal localization. The only exception is the MDS [11], which is shown to work for localization tasks, however, the method is designed primarily for classification. The proposed LAV-DF dataset and method are specifically designed for temporal localization of manipulations.

Temporal Localization. Given that the task of temporal forgery localization is similar to the task of temporal action localization, previous work in this area is important. Benchmark datasets in this domain include THUMOS [25] and ActivityNet [7] and the proposed methods can be grouped into two categories: 2-step structures which first generate segment proposals and then perform multi-class classification to evaluate the proposals [42, 67, 70] and 1-step methods which directly generate the final segment predictions [6, 40, 46]. For the task of temporal forgery localization there are no classification requirements for the foreground segments, that is, the background is always real and the foreground segments are always fake. Therefore, boundary prediction and 1-step methods are more important and related to our task.

Bagchi et al. [2] divided the methods for segment proposal estimation in temporal action localization into two main categories: methods based on anchors and methods based on predicting the boundary probabilities. As for the anchor-based, these methods mainly use sliding windows in the video, such as S-CNN [59], CDC [58], TURN-TAP [18] and CTAP [17]. As for the methods predicting the boundary probabilities, Lin et al. [41] introduced BSN in 2018. The method can utilize the global information to overcome the problem that anchor-based methods cannot generate precise and flexible segment proposals. Based on BSN, BMN [39] and BSN++ [60] were introduced for improved performance. It is worth noting that all these methods are unimodal, which is not optimal for the task of temporal forgery detection. The importance of multimodality was demonstrated recently by AVFusion [2].

Proposed Approach. For the task of temporal forgery detection, both the audio and visual information are important, in addition to the required precise boundary proposals. In this paper, we introduce a multimodal method based on boundary probabilities and compare the performance with BMN [39], AGT [46], MDS [11] and AVFusion [2].

3 LOCALIZED AUDIO VISUAL DEEPFAKE

The proposed dataset is a large audio-visual localised deepfake dataset. The main steps in creating the dataset are: a) Sourcing real videos, b) Processing real videos to manipulate the transcripts and c) Audio and video synthesis. The deepfake generation step is based

Table 1: Quantitative comparison of LAV-DF with previous public deepfake datasets. *Cla*: Classification, *SL*: Spatial Localization, *TFL*: Temporal Forgery Localization, *FS*: Face Swapping, and *RE*: ReEnactment.

Dataset	Year	Tasks	Manipulated Modality	Method Manipulation	#Subjects	#Real	#Fake	#Total
DF-TIMIT [33]	2018	Cla	V	FS	43	320	640	960
UADFV [69]	2019	Cla	V	FS	49	49	49	98
FaceForensics++ [53]	2019	Cla	V	FS/RE	-	1,000	4,000	5,000
Google DFD [48]	2019	Cla	V	FS	-	363	3,068	3,431
DFDC [16]	2020	Cla	AV	FS	960	23,654	104,500	128,154
DeeperForensics [28]	2020	Cla	V	FS	100	50,000	10,000	60,000
Celeb-DF [38]	2020	Cla	V	FS	59	590	5,639	6,229
WildDeepfake [71]	2021	Cla	-	FS	-	3,805	3,509	7,314
FakeAVCeleb [31]	2021	Cla	AV	RE	600+	570	25,000+	25,500+
ForgeryNet [23]	2021	SL/TFL/Cla	V	Random FS/RE	5400+	99,630	121,617	221,247
LAV-DF (Ours)	2022	TFL/Cla	AV	Content driven RE	153	36,431	99,873	136,304

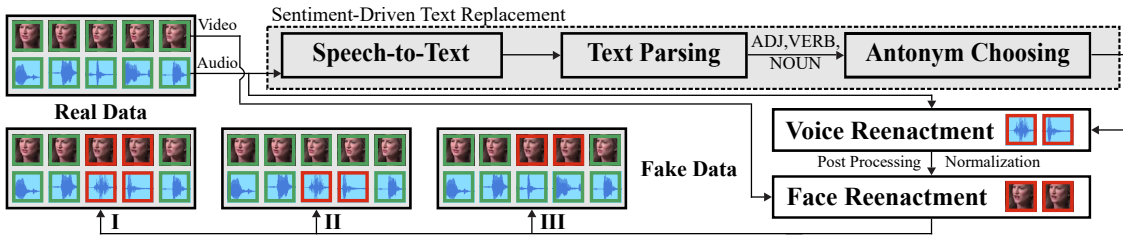


Figure 2: The pipeline for LAV-DF dataset generation. The green-edge audio and video frames are the real data and the red-edge audio and video frames are the generated fake data. The real audio based transcript is used to decide the location and content to be replaced based on the largest change in sentiment. The chosen antonyms are used as an input for generating fake audio with voice cloning. The post-processing and normalization are applied to the audio to maintain the consistency of the loudness between the generated audio and real audio in the neighbourhood. The generated audio is used as input for facial reenactment. Three categories of data are generated: *<Fake Audio and Fake Video>*, *<Fake Audio and Real Video>* and *<Real Audio and Fake Video>*. The details are discussed in Section 3.1.

on the hypothesis that changing relevant word(s) in a statement can lead to change in its perception. The same is also reflected by changing the sentiment value. The manipulation strategy is to replace word/words with its/their antonym(s), which leads to a significant change in the sentiment score of a statement. The overall pipeline of data generation is shown in Figure 2.

Data Source and Parsing. We sourced the real videos from the VoxCeleb2 [12] dataset. VoxCeleb2 is a facial video dataset with over 1 million utterance videos of over 6000 speakers. The videos in VoxCeleb2 are collected from YouTube and the face parts of the video are tracked and cropped by the CNN facial detector in [32] with 224×224 resolution. The original dataset contains videos of different duration, spoken language, and voice loudness. English speaking videos are chosen using the confidence score from Google Speech-to-Text service. The same service generates the transcripts, which are used for manipulation.

3.1 Data Generation

Transcript Manipulation. After collecting and wrangling the real data from VoxCeleb2, the next step is to analyse a video’s transcript denoted by $D = \{d_0, d_1, \dots, d_m, \dots, d_n\}$, where d_i denotes word tokens and n is the number of tokens in the transcript. The aim is to find the tokens to be replaced in D such that the sentiment

score of the transcript changes the most. This is essentially to create transcript $D' = \{d_0, d_1, \dots, d'_m, \dots, d_n\}$, composed of most of the tokens of D with the exception of a few tokens being replaced. These replaced tokens d' are selected from a set \hat{d} of antonyms of d . We used the sentiment analyzer in NLTK [3] which predicts the sentiment value of a video transcript. Positive sentiment value means the sentiment in the transcript $S(D)$ is positive, negative sentiment value means the sentiment is negative, and zero sentiment value means the sentiment is neutral. For each token d in a transcript D , we find the replacement as follows,

$$\tau = \operatorname{argmax}_{d \in D, d' \in \hat{d}} |S(D) - S(D')|$$

We find all the replacements in a transcript D as,

$$\theta = \operatorname{argmax}_{\{\tau_m\}_{m=1}^M} \left| \sum_{i=1}^M \Delta S(\tau_i) \right|$$

where $\Delta S(\tau_i)$ is the sentiment difference with the replacement τ_i and M is the maximum number of replacements in the transcript. For videos shorter than 10 seconds, there is up to 1 replacement; otherwise, there are up to 2 replacements. Figure 3 (a) illustrates the significant change in the sentiment distribution after the manipulations and Figure 3 (b) presents the histogram of $|\Delta S|$, suggesting that the sentiment of most transcripts was successfully changed.

Audio Generation. Once the replacement tokens d' are available, the next step is to generate their corresponding audio in the style of the speaker in the video. We evaluated several recent adaptive TTS methods [9, 27, 47], which can generate the speech style of a person who is not in the training dataset. Based on better performance, we chose speaker verification based multi-speaker TTS (SV2TTS) [27] as the final method for audio generation. The SV2TTS method comprises of three modules: a) An encoder for extracting style embedding of the reference speaker, b) Tacotron 2 [57] based spectrogram generated using the replacement tokens and the speaker style embedding as input, and c) WaveNet [50] based vocoder for generating realistic audio using the spectrogram generated from the synthesizer. We used a pre-trained SV2TTS for generating the fake audio segments and later normalized the loudness of the generated audio using the real audio neighbors.

Video Generation. Once the fake audio is generated, we used it as an input for generating the corresponding fake video frames. We used Wav2Lip facial reenactment [52] for this task as it has been shown to have better output quality than previous methods [26, 29], and has better generalization and robustness to unseen scenarios. It is worth noting that newer methods that achieve better video synthesis quality are not suitable for our task. For example, AD-NeRF [22] is not designed for zero-shot generation of unseen identities and ATVGNet [10] reenacts the face based on a reference static image, which causes pose inconsistencies on the boundary between fake and real segments. Wav2Lip takes a reference video and target audio as input, and generates an output video in which the person in the reference video is speaking the target audio content with synced lips. We used pre-trained Wav2Lip model and up-scaled the generated fake video segment to a resolution of 224×224 . Finally, the generated fake audio and video segments were synchronised and used to replace the original audio and video segments corresponding to the original tokens.

Based on the generation of fake audio and video, we have three variations in the final dataset (similar to [30]):

- 1. Fake Audio and Fake Video.** Both the audio and corresponding video are generated for replacement tokens.
- 2. Fake Audio and Real Video.** Only the audio is generated for replacement tokens and the corresponding real video is length-normalized.
- 3. Real Audio and Fake Video.** Only the video is generated for replacement tokens and the length of the fake video is normalized to match the real audio.

3.2 Dataset Statistics

The dataset contains a total of 136,304 videos of which 36,431 are completely real and 99,873 contain fake segments, with 153 unique identities. We split the dataset into 3 identity independent subsets for training (78703 videos of 91 identities), validation (31501 videos of 31 identities), and testing (26100 videos of 31 identities).

Summary of the dataset is shown in Figure 3. The total number of fake segments is 114,253 with duration in the range [0-1.6] seconds and average length of 0.65 seconds, where 89.26% of the segments are shorter than 1 second. The maximum video length is 20 seconds and 69.61% of the videos are shorter than 10 seconds. As for the

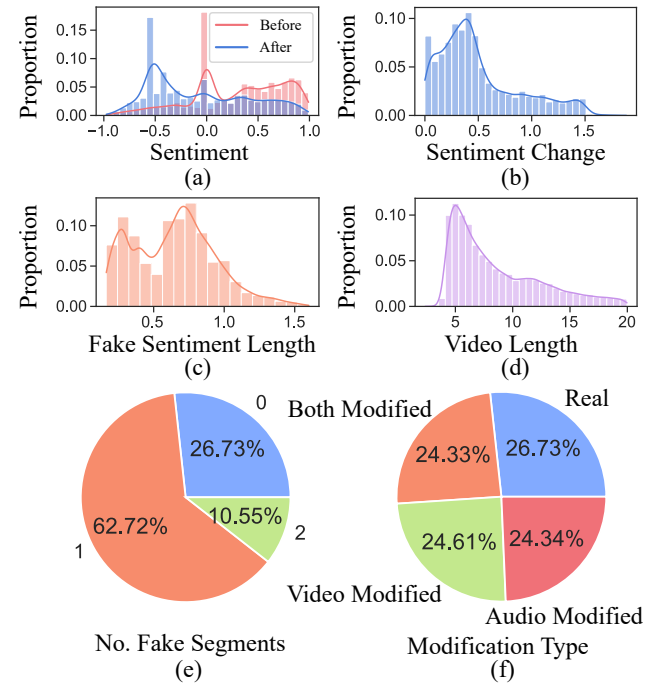


Figure 3: Summary of the LAV-DF dataset: (a) Distribution of sentiment scores, (b) Distribution of sentiment change, (c) Distribution of fake segment lengths, (d) Distribution of video lengths, (e) Proportion of fake segments, and (f) Proportion of modifications.

modality modification types, the amount of the 4 types (i.e. video-modified, audio-modified, both-modified, real) are approximately equal. In most videos (62.72%) there is 1 fake segment, and in some videos (10.55%) there are 2.

4 PROPOSED METHOD

The proposed method Boundary Aware Temporal Forgery Detection (BA-TFD) is illustrated in Figure 4. The first step of the method is to extract features from the input data $X = \{V, A\}$, where V is the video and A is the audio.

4.1 Feature Encoders

Video Encoder. The goal of the video encoder is to learn frame-level spatio-temporal features from the input video V using a 3DCNN. For that purpose we designed the video encoder E_v to take the whole video $V \in \mathbb{R}^{C \times T \times H \times W}$ as input, where T is the number of frames, C is the number of channels, and H and W are the height and width of the frame. The output of the E_v are the frame-level features $F_v \in \mathbb{R}^{C_f \times T}$, where C_f is the features dimension. E_v is composed of 4 blocks, each containing multiple 3D convolutional layers with kernel size $3 \times 3 \times 3$ and a final max-pooling layer.

Audio Encoder. The goal of the audio encoder is to learn features from the input audio A using a 2DCNN. In addition, the learned audio features are temporarily aligned with the learned frame-level video features. The first step is to generate the spectrogram

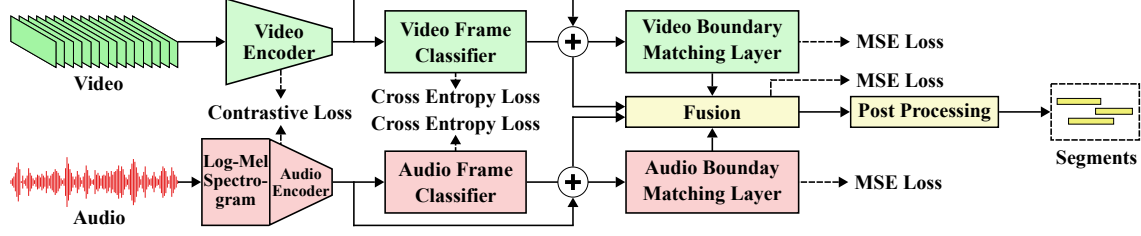


Figure 4: Structure of the proposed method Boundary Aware Temporal Forgery Detection (BA-TFD). The video encoder uses raw video as input. The audio encoder uses spectrograms extracted from raw audio. \oplus denotes concatenation. During inference, post-processing is applied to generate segments from the output of the fusion module. The details are discussed in Section 4.

$A' \in \mathbb{R}^{T_a \times F_m}$ of the audio signal in log-space, where T_a is the temporal dimension and F_m is the length of mel-frequency cepstrum features. In the second step, we designed the audio encoder E_a to take the spectrogram A' as input. The output of the E_a are the audio frame features $F_a \in \mathbb{R}^{C_f \times T}$, where C_f is the features dimension. E_a is composed of multiple 2D convolutional layers with kernel size 3×3 and a final max-pooling layer to reduce the temporal dimension T_a to T .

4.2 Loss Functions

Contrastive Loss. Our hypothesis is that content modification in one or more modalities will result in miss-synchronization between the modalities (i.e. video and audio) and contrastive loss has been shown [11, 13] to be a powerful objective for similar tasks. In our method, the audio and video features learned from real videos are regarded as positive pairs $y = 1$, and the audio and video features learned from videos with at least one modified modality are regarded as negative pairs $y = 0$. For the positive pairs, the contrastive loss minimizes the difference between the modalities while for negative pairs, the contrastive loss keeps that margin larger than δ ,

$$L_c = \frac{1}{NC_f T} \sum_{i=1}^N y_i d_i^2 + (1 - y_i) \max(\delta - d_i, 0)^2$$

$$d_i = \|F_{vi} - F_{ai}\|_2$$

Auxiliary Frame Classification Loss. Since we have access to the frame-level features F_v and F_a , we can utilize the labels and train the encoders to extract powerful and robust features that capture different deepfake artifacts. For that purpose we designed two frame-level logistic regression classifiers FC_v and FC_a using F_v and F_a as input. The classifiers consist of 1D convolutional layers and predict the label \hat{Y} as 1 (fake) or 0 (real) for each frame and each modality. The classifiers are trained with cross-entropy loss,

$$L_f = -\frac{1}{2NT} \sum_{m \in \{a, v\}} \sum_{i=1}^N \sum_{j=1}^T H(\hat{Y}_{mij}, Y_{mij})$$

$$H(\hat{Y}, Y) = Y \log \hat{Y} + (1 - Y) \log (1 - \hat{Y})$$

$$Y_m = \eta_m Y + (1 - \eta_m) Y_0$$

where N is the number of samples in the dataset, T is the number of frames, m is the modality (i.e. audio a or video v), η_m specifies whether modality m is modified, and Y_0 is the label for real videos.

Boundary Matching Loss. The ground truth boundary maps are generated following the procedure in [39]. Given the fusion boundary map \hat{M} , video boundary map \hat{M}_v and audio boundary map \hat{M}_a predicted by the model we use mean squared error as boundary matching loss for \hat{M} , \hat{M}_v and \hat{M}_a . The fusion boundary matching loss is,

$$L_b = \frac{1}{NDT} \sum_{i=1}^N \sum_{j=1}^D \sum_{k=1}^T (\hat{M}_{ijk} - M_{ijk})^2$$

where, N is the number of samples in the dataset, D is the number of all possible proposal durations and T is the number of frames. The modality boundary matching loss is similar to the frame classification loss,

$$L_{bm} = \frac{1}{2NDT} \sum_{m \in \{v, a\}} \sum_{i=1}^N \sum_{j=1}^D \sum_{k=1}^T (\hat{M}_{mijk} - M_{mijk})^2$$

$$M_m = \eta_m M + (1 - \eta_m) M_0$$

where, m is the modality (i.e. video v or audio a), η_m specifies whether modality m is modified, and M_0 is the ground truth boundary map for real videos.

Overall Loss. The overall loss is defined as follows,

$$L = \lambda_c L_c + \lambda_f L_f + \lambda_b L_b + \lambda_{bm} L_{bm}$$

where, λ_c , λ_f , λ_b and λ_{bm} are weights for different losses.

4.3 Multimodal Fusion

The predictions of FC_v and FC_a are concatenated with the features F_v and F_a , and used by two boundary matching layers B_v and B_a [39]. The goal is to predict the boundary maps $\hat{M}_v \in \mathbb{R}^{D \times T}$ and $\hat{M}_a \in \mathbb{R}^{D \times T}$ for the video and audio, where T is the number of frames and D is the maximum duration of the fake segments. The fusion module, illustrated in Figure 5, uses the \hat{M}_v , \hat{M}_a , F_v and F_a as input. For the video modality, the \hat{M}_v , F_v and F_a are used to calculate the video weights $W_v \in \mathbb{R}^{D \times T}$ and for the audio modality, the \hat{M}_a , F_a and F_v are used to calculate the audio weights $W_a \in \mathbb{R}^{D \times T}$. In the final step, we perform element-wise weighted average and calculate the fusion boundary map prediction $\hat{M} \in \mathbb{R}^{D \times T}$,

$$\hat{M} = \frac{W_v \hat{M}_v + W_a \hat{M}_a}{W_v + W_a}$$

where all operations are element-wise.

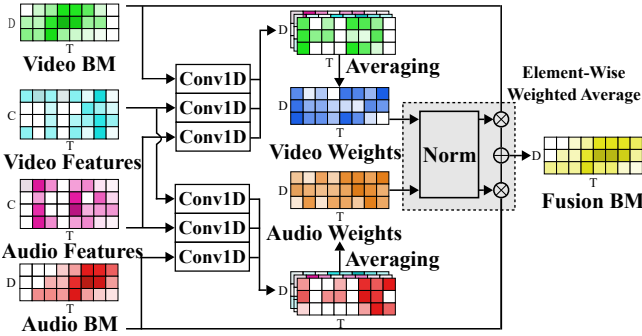


Figure 5: The structure of the fusion module. The gray block normalizes the video and audio weights predicted from the 1D convolutional layers and applies element-wise weighted average. \oplus denotes element-wise addition and \otimes denotes element-wise multiplication. BM: boundary map. For details refer to Section 4.3.

4.4 Inference

During inference, the model uses the video and audio as input and generates a fusion boundary map \hat{M} . The boundary map represents the confidence for all proposals in the video and is very dense (i.e. there are many duplicated proposals). Similar to BSN [41], we utilize post-processing with Soft Non-Maximum Suppression (S-NMS) [4] to eliminate the duplicated proposals.

5 EXPERIMENTS

We have performed extensive benchmarking of LAV-DF via several state-of-the-art methods: BMN [39], AGT [46], AVFusion [2] and MDS [11]. Apart from our proposed dataset LAV-DF, we also validate our method BA-TFD for classification on DFDC dataset.

Dataset Preparation and Evaluation Protocol. To compare with visual-only methods, we prepare a subset of the test set where the audio-only modified data is removed which is denoted as “subset”. The original test set is denoted as “full set” in the experiments.

Unlike temporal action localization methods [42, 46] that are using only average precision, we follow the protocol proposed in ForgeryNet [23] and use both average precision (AP) and average recall (AR) as the evaluation metrics for the quantitative comparison. For AP, we follow the protocol of ActivityNet [7] to set the IoU thresholds to 0.5, 0.75 and 0.95. For AR, as the number of fake segments is small, we set the number of proposals to smaller numbers like 100, 50, 20 and 10 with the IoU thresholds [0.5:0.05:0.95]. Our method can also be used for deepfake detection (i.e. classification) task. We use area under the curve (AUC) for evaluation of the deepfake classification task.

BA-TFD is a multimodal temporal detection method and if only the visual component is used, the method is very similar to BMN. In this work we focus on the problem of temporal localization instead of classification and only DFDC dataset is used to evaluate the classification performance of the proposed method.

Implementation Details. BA-TFD is implemented in PyTorch [51]. For hyperparameters, we set $\lambda_c = 0.1$, $\lambda_f = 2$, $\lambda_b = 1$, $\lambda_{bm} = 1$ and $\delta =$

0.99. For comparison, we trained BMN [39], AGT [46], AVFusion [2] and MDS [11] on temporal forgery localization task.

In addition, to evaluate the usefulness of the proposed method, we compare with MDS, EfficientViT [14] and other methods on classification task. We followed the original settings for BMN, AGT, MDS and EfficientViT, and used encoding concatenation fusion for AVFusion. For the methods that require pre-trained features, we trained them end-to-end with trainable encoder. For comparison, we also trained BMN with I3D features [8] (i.e. fixed encoder). For the models which require S-NMS post-processing, we used the validation set to search for optimal parameters for post-processing. Final evaluation and results are based on the test set.

For DFDC, we consider the whole fake video as one fake segment. For evaluation, we used 2 methods to generate the classification output for BA-TFD: (1) Using the highest confidence of the predicted segments as the confidence of the video being fake and (2) Training a MLP classifier using the confidences of predicted segments. We chose evaluation method (1) for LAV-DF and method (2) for DFDC based on better performance on the datasets.

6 RESULTS

Quantitative Analysis.

Temporal Localization: We compare our model on the LAV-DF full set with the latest methods for temporal action localization and deepfake detection. From Table 2, our model achieves the best performance, which is 76.9 for AP@0.5 and 66.9 for AR@100. Unlike temporal action localization datasets such as ActivityNet, there is a single label for the fake segments, so it is reasonable that the AP score is relatively high. The multimodal MDS is not designed for temporal forgery localization tasks and predicts only fixed length segments (i.e. cannot predict the precise boundaries), hence the scores for that model are low. As for AGT and BMN, the scores are low because they are visual-only unimodal methods and cannot detect the fake segments in videos where only the audio is modified. We also evaluate the visual-only unimodal output of our model, which shows worse results than the multimodal BA-TFD and AVFusion. In addition, the results show that when the video encoder is trained with LAV-DF data, BMN performs significantly better than using I3D features.

We also evaluate those methods on the subset mentioned in Section 5. From Table 3, the performance of the visual-only models is improved, for BA-TFD, the visual-only score improves from 58.55 to 83.55 (AP@0.5) and the margin between unimodal and multimodal is decreased from 18.35 to 1.65 (AP@0.5). Overall, our method still ranks first, which shows that our method has superior performance for temporal forgery detection.

DeepFake Classification: We also compare our method with previous deepfake detection methods on LAV-DF and a subset of DFDC. From Table 5, our model outperforms MDS and EfficientViT on LAV-DF. As for the subset of DFDC, the performance of our method (see Table 6) is better than previous methods such as Meso4 [1] and FWA[37] and is close to MDS. The reasons of BA-TFD performing better in LAV-DF might be several. Our method BA-TFD is not designed and trained for classification task with classification loss. It is trained for temporal forgery localization and then the segment outputs are summarized as a whole video label prediction.

Table 2: Temporal forgery localization results on the full set (please see Section 5) of LAV-DF. The BA-TFD (visual-only) is the output from video boundary matching layer in Figure 4, showing the performance when using only the video modality.

Model	AP@0.5	AP@0.75	AP@0.95	AR@100	AR@50	AR@20	AR@10
MDS [11]	12.78	01.62	00.00	37.88	36.71	34.39	32.15
AGT [46]	17.85	09.42	00.11	43.15	34.23	24.59	16.71
BMN [39]	24.01	07.61	00.07	53.26	41.24	31.60	26.93
BMN (I3D)	10.56	01.66	00.00	48.49	44.39	37.13	31.55
AVFusion [2]	65.38	23.89	00.11	62.98	59.26	54.80	52.11
BA-TFD (visual-only)	58.55	28.60	00.16	62.49	58.77	53.86	50.29
BA-TFD	76.90	38.50	00.25	66.90	64.08	60.77	58.42

Table 3: Temporal forgery localization results on the subset (please see Section 5) of LAV-DF. The BA-TFD (visual-only) is the output from video boundary matching layer in Figure 4, showing the performance when using only the video modality.

Model	AP@0.5	AP@0.75	AP@0.95	AR@100	AR@50	AR@20	AR@10
MDS [11]	23.43	03.48	00.00	58.53	56.68	53.16	49.67
AGT [46]	15.69	10.69	00.15	49.11	40.31	31.70	23.13
BMN [39]	32.32	11.38	00.14	59.69	48.17	39.01	34.17
BMN (I3D)	28.10	05.47	00.01	55.49	54.44	52.14	47.72
AVFusion [2]	62.01	22.77	00.11	61.98	58.08	53.31	50.52
BA-TFD (visual-only)	83.55	41.88	00.24	65.79	62.30	57.95	55.34
BA-TFD	85.20	47.06	00.29	67.34	64.52	61.19	59.32

Table 4: Temporal forgery localization results of BA-TFD with different losses.

Loss Function	AP@0.5	AP@0.75	AP@0.95	AR@100	AR@50	AR@20	AR@10
L_b	53.16	11.91	00.02	53.99	50.94	47.74	45.55
L_{bm}, L_b	54.70	15.50	00.04	56.64	53.57	49.46	45.85
L_f, L_{bm}, L_b	76.50	39.92	00.18	66.69	63.71	60.07	57.76
L_c, L_f, L_{bm}, L_b	76.90	38.50	00.25	66.90	64.08	60.77	58.42

Therefore, the performance of our method drops as compared to the state-of-the-art classification method MDS. On the other hand, previous deepfake detection methods assume that fake videos are entirely fake, so their performance is reduced on LAV-DF. In summary, our method still performs well on classification task and has potential to reach the state-of-the-art performance.

Impact of Loss Functions: To examine the contributions of each loss of BA-TFD, we train four models with different combinations of losses. From Table 4, all four losses have positive influences on the performance. By observing the difference between the scores, the frame classification loss L_c contributes the most in the model. With the frame-level label supervising the model, the encoders are trained to have a better capacity to extract the features relevant to deepfake artifacts. We visualize the distributions of video features F_v of 10 videos in the dataset in Figure 7. From the plots, with frame classification loss and contrastive loss added, the features are more separable, which contributes to the temporal localization and improves the performance.

Qualitative Analysis. We selected a real video sample and three corresponding fake videos each with manipulation in a single or both modalities. For these four videos, we visualize the boundary map outputs \hat{M}_v , \hat{M}_a and \hat{M} in Figure 6. It is observed that the video output captures the fake segments when the video modality

is manipulated. The same holds for audio. Regardless of whether the audio or video modality is modified, the fusion output captures the correct information from audio and visual outputs and shows the effectiveness of the fusion module.

Failure Analysis. We observe that BA-TFD predictions can be noisy in a few cases, which contain only a short duration (≤ 0.5 sec) video manipulations and the corresponding real audio. We argue that for such short video-only manipulations, if the visual transition from real to fake and then to real is smooth, it may lead to a noisy result.

7 CONCLUSION, LIMITATION AND FUTURE WORK

In this work we investigated the problem of deepfake detection from the perspective of partial video modification. To this end, a new dataset LAV-DF is curated in which the audio and video are modified at specific locations based on the potential change in sentiment of the video content. For this problem, we also proposed a new method BA-TFD. The conducted experiments show that our method achieves better performance than previous relevant state-of-the-art methods.

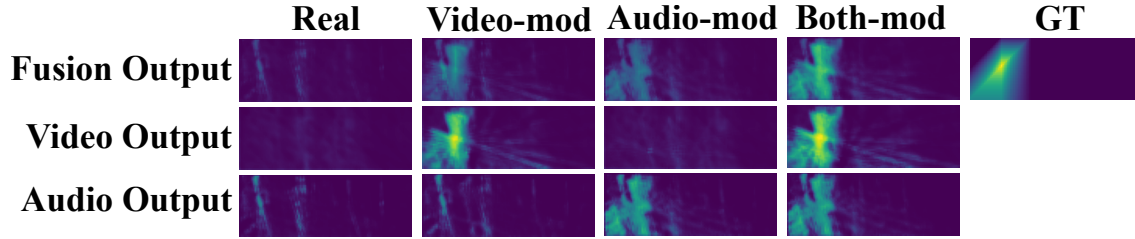


Figure 6: Boundary map output visualizations. The first column illustrates the modality-wise boundary map outputs for a *real* video. The other columns illustrate the modality-wise boundary map outputs of the corresponding *fake* videos (i.e. video based modification, audio based modification and audio-visual based modification). *mod*: modified and *GT*: ground truth.

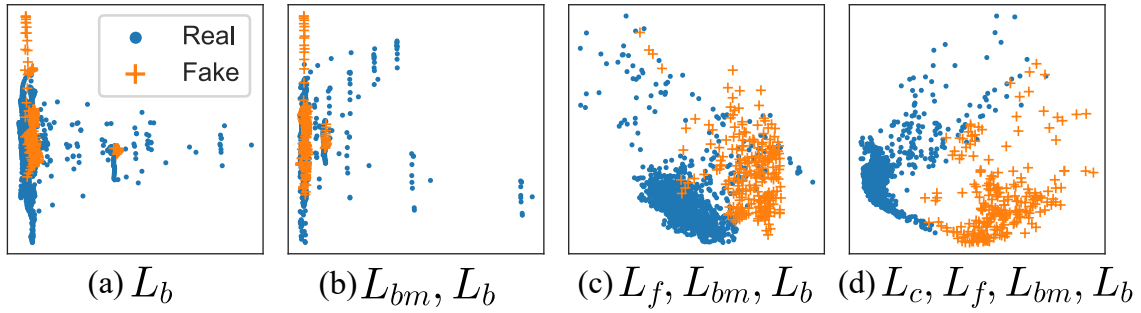


Figure 7: Feature distribution in PCA subspace. Each point is the features of a video frame marked with real or fake.

Table 5: Classification results on the full set of LAV-DF.

Dataset		LAV-DF		
Model	MDS [11]	EfficientViT [14]	BA-TFD	
AUC	0.828	0.965	0.990	

Table 6: Classification results on a subset set of DFDC.

Dataset		DFDC				
Model	Meso4[1]	FWA[37]	Siamese[44]	MDS [11]	BA-TFD	
AUC	0.753	0.727	0.844	0.916	0.846	

Potential Risks and Ethical Concerns. Our work especially LAV-DF might include potential negative social impacts. As the subjects in the dataset are celebrities, the content in the dataset may be used for unethical purposes such as making fake rumours. Also, the dataset generation pipeline can be applied to create fake videos. To encounter the negative impacts, we prepared a license for public usage of the dataset and proposed the BA-TFD.

Limitations. Major limitations are: a) The audio reenactment method used in the dataset does not always generate the reference style and b) The resolution of the dataset is constrained on the basis of source videos.

Future work. Major improvement in the future will be increasing LAV-DF with new token insertion, substitution and deletion of existing tokens and converting statements into questions.

REFERENCES

- [1] Darius Afchar, Vincent Nozick, Junichi Yamagishi, and Isao Echizen. 2018. MesoNet: a Compact Facial Video Forgery Detection Network. In *2018 IEEE International Workshop on Information Forensics and Security (WIFS)*. 1–7. <https://doi.org/10.1109/WIFS.2018.8630761> ISSN: 2157-4774.
- [2] Anurag Bagchi, Jazib Mahmood, Dolton Fernandes, and Ravi Kiran Sarvadevabhatla. 2021. Hear Me Out: Fusional Approaches for Audio Augmented Temporal Action Localization. *arXiv:2106.14118 [cs]* (Aug. 2021). arXiv: 2106.14118 version: 3.
- [3] Steven Bird, Ewan Klein, and Edward Loper. 2009. *Natural Language Processing with Python: Analyzing Text with the Natural Language Toolkit*. O'Reilly Media, Inc. Google-Books-ID: KG1fbuP1i4C.
- [4] Navaneeth Bodla, Bharat Singh, Rama Chellappa, and Larry S. Davis. 2017. Soft-NMS – Improving Object Detection With One Line of Code. In *Proceedings of the IEEE International Conference on Computer Vision*. 5561–5569.
- [5] John Brandon. 2019. There Are Now 15,000 Deepfake Videos on Social Media. Yes, You Should Worry. *Forbes* (Oct. 2019).
- [6] Shyamal Buch, Victor Escorcia, Bernard Ghanem, Li Fei-Fei, and Juan Carlos Niebles. 2019. End-to-end, single-stream temporal action detection in untrimmed videos. *Proceedings of the British Machine Vision Conference 2017* (May 2019). <https://doi.org/10.5244/c.31.93> Publisher: British Machine Vision Association.
- [7] Fabian Caba Heilbron, Victor Escorcia, Bernard Ghanem, and Juan Carlos Niebles. 2015. ActivityNet: A Large-Scale Video Benchmark for Human Activity Understanding. In *Proceedings of the IEEE Conference on Computer Vision and Pattern Recognition*. 961–970.
- [8] Joao Carreira and Andrew Zisserman. 2017. Quo Vadis, Action Recognition? A New Model and the Kinetics Dataset. In *Proceedings of the IEEE Conference on Computer Vision and Pattern Recognition*. 6299–6308.
- [9] Edresson Casanova, Christopher Shulby, Eren Gölge, Nicolas Michael Müller, Frederico Santos de Oliveira, Arnaldo Cândido Junior, Anderson da Silva Soares, Sandra Maria Aluísio, and Moacir Antonelli Ponti. 2021. SC-GlowTTS: an Efficient Zero-Shot Multi-Speaker Text-To-Speech Model. *arXiv:2104.05557 [cs, eess]* (June 2021). arXiv: 2104.05557.
- [10] Lele Chen, Ross K. Maddox, Zhiyao Duan, and Chenliang Xu. 2019. Hierarchical Cross-Modal Talking Face Generation With Dynamic Pixel-Wise Loss. In *Proceedings of the IEEE/CVF Conference on Computer Vision and Pattern Recognition*. 7832–7841.
- [11] Komal Chugh, Parul Gupta, Abhinav Dhall, and Ramanathan Subramanian. 2020. Not made for each other- Audio-Visual Dissonance-based Deepfake Detection

and Localization. In *Proceedings of the 28th ACM International Conference on Multimedia (MM '20)*. Association for Computing Machinery, New York, NY, USA, 439–447. <https://doi.org/10.1145/3394171.3413700>

[12] J. S. Chung, A. Nagrani, and A. Zisserman. 2018. VoxCeleb2: Deep Speaker Recognition. In *INTERSPEECH*.

[13] Joon Son Chung and Andrew Zisserman. 2017. Out of Time: Automated Lip Sync in the Wild. In *Computer Vision – ACCV 2016 Workshops (Lecture Notes in Computer Science)*, Chu-Song Chen, Jiwen Lu, and Kai-Kuang Ma (Eds.). Springer International Publishing, Cham, 251–263. https://doi.org/10.1007/978-3-319-54427-4_19

[14] Davide Coccimini, Nicola Messina, Claudio Gennaro, and Fabrizio Falchi. 2021. Combining EfficientNet and Vision Transformers for Video Deepfake Detection. *arXiv:2107.02612 [cs]* (July 2021). arXiv: 2107.02612 version: 1.

[15] Oscar de Lima, Sean Franklin, Shreshtha Basu, Blake Karwoski, and Annet George. 2020. Deepfake Detection using Spatiotemporal Convolutional Networks. *arXiv:2006.14749 [cs, eess]* (June 2020). arXiv: 2006.14749.

[16] Brian Dolhansky, Joanna Bitton, Ben Pflaum, Jikuo Lu, Russ Howes, Menglin Wang, and Cristian Canton Ferrer. 2020. The DeepFake Detection Challenge (DFDC) Dataset. *arXiv:2006.07397 [cs]* (Oct. 2020). arXiv: 2006.07397.

[17] Jiyang Gao, Kan Chen, and Ram Nevatia. 2018. CTAP: Complementary Temporal Action Proposal Generation. In *Proceedings of the European Conference on Computer Vision (ECCV)*. 68–83.

[18] Jiyang Gao, Zhenheng Yang, Kan Chen, Chen Sun, and Ram Nevatia. 2017. TURN TAP: Temporal Unit Regression Network for Temporal Action Proposals. In *Proceedings of the IEEE International Conference on Computer Vision*. 3628–3636.

[19] Ian Goodfellow, Jean Pouget-Abadie, Mehdi Mirza, Bing Xu, David Warde-Farley, Sherjil Ozair, Aaron Courville, and Yoshua Bengio. 2020. Generative adversarial networks. *Commun. ACM* 63, 11 (Oct. 2020), 139–144. <https://doi.org/10.1145/3422622>

[20] Zhihao Gu, Yang Chen, Taiping Yao, Shouhong Ding, Jilin Li, Feiyue Huang, and Lizhuang Ma. 2021. *Spatiotemporal Inconsistency Learning for DeepFake Video Detection*. Association for Computing Machinery, New York, NY, USA, 3473–3481. <https://doi.org.ezproxy.lib.monash.edu.au/10.1145/3474085.3475508>

[21] Luca Guarnera, Oliver Giudice, and Sebastiano Battiatto. 2020. DeepFake Detection by Analyzing Convolutional Traces. In *Proceedings of the IEEE/CVF Conference on Computer Vision and Pattern Recognition Workshops*. 666–667.

[22] Yudong Guo, Keyu Chen, Sen Liang, Yong-Jin Liu, Hujun Bao, and Juyong Zhang. 2021. AD-NeRF: Audio Driven Neural Radiance Fields for Talking Head Synthesis. In *Proceedings of the IEEE/CVF International Conference on Computer Vision*. 5784–5794.

[23] Yinan He, Bei Gan, Siyu Chen, Yichun Zhou, Guojun Yin, Luchuan Song, Lu Sheng, Jing Shao, and Ziwei Liu. 2021. ForgeryNet: A Versatile Benchmark for Comprehensive Forgery Analysis. In *Proceedings of the IEEE/CVF Conference on Computer Vision and Pattern Recognition*. 4360–4369.

[24] Young-Jin Heo, Young-Ju Choi, Young-Woon Lee, and Byung-Gyu Kim. 2021. Deepfake Detection Scheme Based on Vision Transformer and Distillation. *arXiv:2104.01353 [cs]* (April 2021). arXiv: 2104.01353.

[25] Haroon Idrees, Amir R. Zamir, Yu-Gang Jiang, Alex Gorban, Ivan Laptev, Rahul Sukthankar, and Mubarak Shah. 2017. The THUMOS Challenge on Action Recognition for Videos “in the Wild”. *Computer Vision and Image Understanding* 155 (Feb. 2017), 1–23. <https://doi.org/10.1016/j.cviu.2016.10.018> arXiv: 1604.06182.

[26] Amir Jamaludin, Joon Son Chung, and Andrew Zisserman. 2019. You Said That?: Synthesizing Talking Faces from Audio. *International Journal of Computer Vision* 127, 11 (Dec. 2019), 1767–1779. <https://doi.org/10.1007/s11263-019-01150-y>

[27] Ye Jia, Yu Zhang, Ron J. Weiss, Quan Wang, Jonathan Shen, Fei Ren, Zhifeng Chen, Patrick Nguyen, Ruoming Pang, Ignacio Lopez Moreno, and Yonghui Wu. 2018. Transfer learning from speaker verification to multispeaker text-to-speech synthesis. In *Proceedings of the 32nd International Conference on Neural Information Processing Systems (NIPS'18)*. Curran Associates Inc., Red Hook, NY, USA, 4485–4495.

[28] Liming Jiang, Ren Li, Wayne Wu, Chen Qian, and Chen Change Loy. 2020. DeepForensics-1.0: A Large-Scale Dataset for Real-World Face Forgery Detection. In *Proceedings of the IEEE/CVF Conference on Computer Vision and Pattern Recognition*. 2889–2898.

[29] Prajwal K R, Rudrabha Mukhopadhyay, Jerin Philip, Abhishek Jha, Vinay Namboodiri, and C V Jawahar. 2019. Towards Automatic Face-to-Face Translation. In *Proceedings of the 27th ACM International Conference on Multimedia (MM '19)*. Association for Computing Machinery, New York, NY, USA, 1428–1436. <https://doi.org/10.1145/3343031.3351066>

[30] Hasam Khalid, Minho Kim, Shahroz Tariq, and Simon S. Woo. 2021. Evaluation of an Audio-Video Multimodal Deepfake Dataset using Unimodal and Multimodal Detectors. *Proceedings of the 1st Workshop on Synthetic Multimedia - Audiovisual Deepfake Generation and Detection* (Oct. 2021), 7–15. <https://doi.org/10.1145/3476099.3484315> arXiv: 2109.02993.

[31] Hasam Khalid, Shahroz Tariq, and Simon S. Woo. 2021. FakeAVCeleb: A Novel Audio-Video Multimodal Deepfake Dataset. *arXiv:2108.05080 [cs]* (Aug. 2021). arXiv: 2108.05080.

[32] Davis E. King. 2009. Dlib-ml: A Machine Learning Toolkit. *The Journal of Machine Learning Research* 10 (Dec. 2009), 1755–1758.

[33] Pavel Korshunov and Sébastien Marcel. 2018. DeepFakes: a New Threat to Face Recognition? Assessment and Detection. *arXiv:1812.08685 [cs]* (Dec. 2018). arXiv: 1812.08685.

[34] Iryna Korshunova, Wenzhe Shi, Joni Dambre, and Lucas Theis. 2017. Fast Face-Swap Using Convolutional Neural Networks. In *Proceedings of the IEEE International Conference on Computer Vision*. 3677–3685.

[35] Trung-Nghia Le, Huy H. Nguyen, Junichi Yamagishi, and Isao Echizen. 2021. OpenForensics: Large-Scale Challenging Dataset for Multi-Face Forgery Detection and Segmentation In-the-Wild. In *Proceedings of the IEEE/CVF International Conference on Computer Vision*. 10117–10127.

[36] John K. Lewis, Imad Eddine Toubal, Helen Chen, Vishal Sandesara, Michael Lomnitz, Zigfried Hampel-Arias, Calyam Prasad, and Kannappan Palaniappan. 2020. Deepfake Video Detection Based on Spatial, Spectral, and Temporal Inconsistencies Using Multimodal Deep Learning. In *2020 IEEE Applied Imagery Pattern Recognition Workshop (AIPR)*. 1–9. <https://doi.org/10.1109/AIPR50011.2020.9425167> ISSN: 2332-5615.

[37] Yuezun Li and Siwei Lyu. 2019. Exposing DeepFake Videos By Detecting Face Warping Artifacts. In *IEEE Conference on Computer Vision and Pattern Recognition Workshops (CVPRW)*. 7.

[38] Yuezun Li, Xin Yang, Pu Sun, Honggang Qi, and Siwei Lyu. 2020. Celeb-DF: A Large-Scale Challenging Dataset for DeepFake Forensics. In *Proceedings of the IEEE/CVF Conference on Computer Vision and Pattern Recognition*. 3207–3216.

[39] Tianwei Lin, Xiao Liu, Xin Li, Errui Ding, and Shilei Wen. 2019. BMN: Boundary-Matching Network for Temporal Action Proposal Generation. In *Proceedings of the IEEE/CVF International Conference on Computer Vision*. 3889–3898.

[40] Tianwei Lin, Xu Zhao, and Zheng Shou. 2017. Single Shot Temporal Action Detection. In *Proceedings of the 25th ACM international conference on Multimedia (MM '17)*. Association for Computing Machinery, New York, NY, USA, 988–996. <https://doi.org/10.1145/3123266.3123343>

[41] Tianwei Lin, Xu Zhao, Haisheng Su, Chongjing Wang, and Ming Yang. 2018. BSN: Boundary Sensitive Network for Temporal Action Proposal Generation. In *Proceedings of the European Conference on Computer Vision (ECCV)*. 3–19.

[42] Xiaolong Liu, Yao Hu, Song Bai, Fei Ding, Xiang Bai, and Philip H. S. Torr. 2021. Multi-Shot Temporal Event Localization: A Benchmark. In *Proceedings of the IEEE/CVF Conference on Computer Vision and Pattern Recognition*. 12596–12606.

[43] Yisroel Mirsky and Wenke Lee. 2021. The Creation and Detection of Deepfakes: A Survey. *Comput. Surveys* 54, 1 (Jan. 2021), 7:1–7:41. <https://doi.org/10.1145/3425780>

[44] Trisha Mittal, Uttaran Bhattacharya, Rohan Chandra, Aniket Bera, and Dinesh Manocha. 2020. Emotions Don’t Lie: An Audio-Visual Deepfake Detection Method using Affective Cues. In *Proceedings of the 28th ACM International Conference on Multimedia (MM '20)*. Association for Computing Machinery, New York, NY, USA, 2823–2832. <https://doi.org/10.1145/3394171.3413570>

[45] Daniel Mas Montserrat, Hanxiang Hao, Sri K. Yarlagadda, Sriram Baigareddy, Ruiting Shao, Janos Horvath, Emily Bartusiaik, Justin Yang, David Guera, Fengqing Zhu, and Edward J. Delp. 2020. Deepfakes Detection With Automatic Face Weighting. In *Proceedings of the IEEE/CVF Conference on Computer Vision and Pattern Recognition Workshops*. 668–669.

[46] Megha Nawhal and Greg Mori. 2021. Activity Graph Transformer for Temporal Action Localization. *arXiv:2101.08540 [cs]* (Jan. 2021). arXiv: 2101.08540.

[47] Paarth Neekhara, Shehzain Hussain, Shlomo Dubnov, Farinaz Koushanfar, and Julian McAuley. 2021. Expressive Neural Voice Cloning. *arXiv:2102.00151 [cs, eess]* (Jan. 2021). arXiv: 2102.00151.

[48] Dufouf Nick and Jigsaw Andrew. 2019. Contributing Data to Deepfake Detection Research.

[49] Yuval Nirkin, Yosi Keller, and Tal Hassner. 2019. FSGAN: Subject Agnostic Face Swapping and Reenactment. In *Proceedings of the IEEE/CVF International Conference on Computer Vision*. 7184–7193.

[50] Aaron van den Oord, Sander Dieleman, Heiga Zen, Karen Simonyan, Oriol Vinyals, Alex Graves, Nal Kalchbrenner, Andrew Senior, and Koray Kavukcuoglu. 2016. WaveNet: A Generative Model for Raw Audio. *arXiv:1609.03499 [cs]* (Sept. 2016). arXiv: 1609.03499.

[51] Adam Paszke, Sam Gross, Francisco Massa, Adam Lerer, James Bradbury, Gregory Chanan, Trevor Killeen, Zeming Lin, Natalia Gimelshein, Luca Antiga, Alban Desmaison, Andreas Kopf, Edward Yang, Zachary DeVito, Martin Raison, Alykhan Tejani, Sasank Chilamkurthy, Benoit Steiner, Lu Fang, Junjie Bai, and Soumith Chintala. 2019. PyTorch: An Imperative Style, High-Performance Deep Learning Library. In *Advances in Neural Information Processing Systems*, Vol. 32. Curran Associates, Inc.

[52] K R Prajwal, Rudrabha Mukhopadhyay, Vinay P. Namboodiri, and C V Jawahar. 2020. A Lip Sync Expert Is All You Need for Speech to Lip Generation In the Wild. In *Proceedings of the 28th ACM International Conference on Multimedia (MM '20)*. Association for Computing Machinery, New York, NY, USA, 484–492. <https://doi.org/10.1145/3394171.3413532>

[53] Andreas Rossler, Davide Cozzolino, Luisa Verdoliva, Christian Riess, Justus Thies, and Matthias Niessner. 2019. FaceForensics++: Learning to Detect Manipulated

Facial Images. In *Proceedings of the IEEE/CVF International Conference on Computer Vision*. 1–11.

[54] David E. Rumelhart, Geoffrey E. Hinton, and Ronald J. Williams. 1985. *Learning Internal Representations by Error Propagation*. Technical Report, CALIFORNIA UNIV SAN DIEGO LA JOLLA INST FOR COGNITIVE SCIENCE. Section: Technical Reports.

[55] Ian Sample. 2020. What are deepfakes – and how can you spot them? *The Guardian* (Jan. 2020).

[56] Oscar Schwartz. 2018. You thought fake news was bad? Deep fakes are where truth goes to die. *The Guardian* (Nov. 2018).

[57] Jonathan Shen, Ruoming Pang, Ron J. Weiss, Mike Schuster, Navdeep Jaitly, Zongheng Yang, Zhifeng Chen, Yu Zhang, Yuxuan Wang, Rj Skerrv-Ryan, Rif A. Saurous, Yannis Agiomvrgiannakis, and Yonghui Wu. 2018. Natural TTS Synthesis by Conditioning Wavenet on MEL Spectrogram Predictions. In *2018 IEEE International Conference on Acoustics, Speech and Signal Processing (ICASSP)*. 4779–4783. <https://doi.org/10.1109/ICASSP.2018.8461368> ISSN: 2379-190X.

[58] Zheng Shou, Jonathan Chan, Alireza Zareian, Kazuyuki Miyazawa, and Shih-Fu Chang. 2017. CDC: Convolutional-De-Convolutional Networks for Precise Temporal Action Localization in Untrimmed Videos. In *Proceedings of the IEEE Conference on Computer Vision and Pattern Recognition*. 5734–5743.

[59] Zheng Shou, Dongang Wang, and Shih-Fu Chang. 2016. Temporal Action Localization in Untrimmed Videos via Multi-Stage CNNs. In *Proceedings of the IEEE Conference on Computer Vision and Pattern Recognition*. 1049–1058.

[60] Haisheng Su, Weihao Gan, Wei Wu, Yu Qiao, and Junjie Yan. 2021. BSN++: Complementary Boundary Regressor with Scale-Balanced Relation Modeling for Temporal Action Proposal Generation. *arXiv:2009.07641 [cs]* (March 2021). arXiv: 2009.07641.

[61] Justus Thies, Mohamed Elgharib, Ayush Tewari, Christian Theobalt, and Matthias Nießner. 2020. Neural Voice Puppetry: Audio-Driven Facial Reenactment. In *ECCV 2020 (Lecture Notes in Computer Science)*, Andrea Vedaldi, Horst Bischof, Thomas Brox, and Jan-Michael Frahm (Eds.). Springer International Publishing, Cham, 716–731. https://doi.org/10.1007/978-3-030-58517-4_42

[62] Daniel Thomas. 2020. Deepfakes: A threat to democracy or just a bit of fun? *BBC News* (Jan. 2020).

[63] Sergey Tulyakov, Ming-Yu Liu, Xiaodong Yang, and Jan Kautz. 2018. MoCoGAN: Decomposing Motion and Content for Video Generation. In *Proceedings of the IEEE Conference on Computer Vision and Pattern Recognition*. 1526–1535.

[64] Junke Wang, Zuxuan Wu, Jingjing Chen, and Yu-Gang Jiang. 2021. M2TR: Multi-modal Multi-scale Transformers for Deepfake Detection. *arXiv:2104.09770 [cs]* (April 2021). arXiv: 2104.09770.

[65] Yuxuan Wang, R. J. Skerry-Ryan, Daisy Stanton, Yonghui Wu, Ron J. Weiss, Navdeep Jaitly, Zongheng Yang, Ying Xiao, Zhifeng Chen, Samy Bengio, Quoc Le, Yannis Agiomvrgiannakis, Rob Clark, and Rif A. Saurous. 2017. Tacotron: Towards End-to-End Speech Synthesis. *arXiv:1703.10135 [cs]* (April 2017). arXiv: 1703.10135.

[66] Deressa Wodajo and Solomon Atnafu. 2021. Deepfake Video Detection Using Convolutional Vision Transformer. *arXiv:2102.11126 [cs]* (March 2021). arXiv: 2102.11126.

[67] Mengmeng Xu, Chen Zhao, David S. Rojas, Ali Thabet, and Bernard Ghanem. 2020. G-TAD: Sub-Graph Localization for Temporal Action Detection. In *Proceedings of the IEEE/CVF Conference on Computer Vision and Pattern Recognition*. 10156–10165.

[68] Ke Yang, Peng Qiao, Dongsheng Li, Shaohe Lv, and Yong Dou. 2018. Exploring Temporal Preservation Networks for Precise Temporal Action Localization. *Proceedings of the AAAI Conference on Artificial Intelligence* 32, 1 (April 2018). Number: 1.

[69] Xin Yang, Yuezun Li, and Siwei Lyu. 2019. Exposing Deep Fakes Using Inconsistent Head Poses. In *ICASSP 2019 - 2019 IEEE International Conference on Acoustics, Speech and Signal Processing (ICASSP)*. 8261–8265. <https://doi.org/10.1109/ICASSP.2019.8683164> ISSN: 2379-190X.

[70] Runhao Zeng, Wenbing Huang, Mingkui Tan, Yu Rong, Peilin Zhao, Junzhou Huang, and Chuang Gan. 2019. Graph Convolutional Networks for Temporal Action Localization. In *Proceedings of the IEEE/CVF International Conference on Computer Vision*. 7094–7103.

[71] Bojia Zi, Minghao Chang, Jingjing Chen, Xingjun Ma, and Yu-Gang Jiang. 2020. WildDeepfake: A Challenging Real-World Dataset for Deepfake Detection. In *Proceedings of the 28th ACM International Conference on Multimedia (MM '20)*. Association for Computing Machinery, New York, NY, USA, 2382–2390. <https://doi.org/10.1145/3394171.3413769>